

## Ion Channels from Linear and Branched Bola-Amphiphiles

P. K. Eggers, T. M. Fyles,\* K. D. D. Mitchell, and T. Sutherland

Department of Chemistry, University of Victoria, Victoria, British Columbia, V8W 3P6, Canada

tmf@uvic.ca

Received September 7, 2002

The synthesis and characterization of the ion channel activity of three new bola-amphiphiles is described. These compounds are conceptually derived from a previously reported bis-cyclophane bola-amphiphile through opening of the cyclophanes to acyclic structures and were found to readily form ion channels in planar bilayer membranes as assessed by bilayer clamp single-channel analysis. All three compounds behaved very similarly: the dominant channels formed by all three are Ohmic with specific conductance of  $10 \pm 1$  pS (NaCl electrolyte) and  $39 \pm 1$  pS (CsCl electrolyte). Single-ion permeability ratios, determined from dissymmetric electrolyte experiments, showed the selectivity  $P(\text{Cs}^+) > P(\text{Na}^+) > P(\text{Cl}^-)$ . Less frequently, lower conductance channels were also observed to act independently of the dominant channels. The lifetimes of the dominant channels range from 70 to 280 ms for the three compounds with some very long-lived openings (20–40 s) observed for two of the three. The lower conductance states have shorter lifetimes. This study demonstrates that bis-macrocyclic compounds are not essential for channel formation by bola-amphiphiles, and opens a new class of channel-forming compounds for structure–activity optimization.

Electrical signaling in sensory and motor neurons depends on the control and manipulation of transmembrane ionic gradients. This is achieved by ion channel proteins that display ionic selectivity, current rectification, and receptor gating functions that combine to transfer the signal along the neuron.<sup>1,2</sup> If such processes could be reproduced in an abiological context, they would lead directly to sensor applications<sup>3</sup> and potentially to novel systems for propagation and processing of signals.<sup>4,5</sup> There have been two main thrusts in the development of such artificial ion channels: the modification of naturally occurring compounds through semisynthesis to alter or control preexisting channel behavior<sup>6–9</sup> and the design and total synthesis of ion channel forming compounds (for reviews, see refs 10–13; for recent papers, see refs 14–18) The latter strategy has produced a wide range

of structural archetypes, many of which generate functionally competent ion channels. Simple structural variations of each of these active channels can alter the activity, selectivity,<sup>19</sup> and ultimately the rectification of the ionic current,<sup>20–23</sup> indicating that the transport process can be brought under direct structural control. A weakness of both approaches to artificial ion channels is the synthetic challenges of published syntheses: many reported materials are destined to remain as laboratory curiosities due to lengthy and inefficient syntheses.

A potential solution to the problem of synthetic complexity lies in a dramatic simplification of the structures. We recently reported on the channels formed by very simple isophthalic acid derivatives.<sup>24</sup> Although channel activity was clearly evident, these structures are probably

\* Corresponding author. Tel: (250) 721 7150. Fax: (250) 721 7147.

(1) Hille, B. *Ionic Channels of Excitable Membranes*, 2nd ed.; Sinauer Assoc.: Sunderland, MA, 1992.

(2) Sargent, P. B. *An Introduction to Molecular Neurobiology*; Hall, Z. W., Ed.; Sinauer Assoc.: Sunderland, MA, 1992; pp 33–80.

(3) Cheng, Y. L.; Bushby, R. J.; Evans, S. D.; Knowles, P. F.; Miles, R. E.; Ogier, S. D. *Langmuir* **2001**, *17*, 1240–1242.

(4) Rentschler, M.; Fromherz, P. *Langmuir* **1998**, *14*, 547–551.

(5) Lahiri, J.; Kalal, P.; Frutos, A. G.; Jonas, S. T.; Schaeffler, R. *Langmuir* **2000**, *16*, 7805–7810.

(6) Koeppe, R. E.; Andersen, O. S. *Annu. Rev. Biophys. Biomol. Struct.* **1996**, *25*, 231–258.

(7) Woolley, G. A.; Zunic, V.; Karanicolas, J.; Jaikaran, A. S. I.; Starostin, A. V. *Biophys. J.* **1997**, *73*, 2465–2475.

(8) Borisenko, V.; Sansom, M. S. P.; Woolley, G. A. *Biophys. J.* **2000**, *78*, 1335–1348.

(9) Schrey, A.; Vescovi, A.; Knoll, A.; Rickert, C.; Koert, U. *Angew. Chem., Int. Ed. Eng.* **2000**, *39*, 900.

(10) Fyles, T. M.; van Straaten-Nijenhuis, W. F. *Comprehensive Supramolecular Chemistry*; Reinhoudt, D. N., Ed.; Elsevier Science: Amsterdam/New York, 1996; Vol. 10, pp 53–77.

(11) Kobuke, Y. *Advances in Supramolecular Chemistry*; Gokel, G. W., Ed.; JAI Press: Greenwich, CT, 1997; Vol. 4, pp 163–210.

(12) Gokel, G. W.; Mukhopadhyay, A. *Chem. Soc. Rev.* **2001**, *30*, 274–286.

(13) Matile, S. *Chem. Soc. Rev.* **2001**, *30*, 158–167.

(14) Otto, S.; Osifchin, M.; Regen, S. L. *J. Am. Chem. Soc.* **1999**, *121*, 7276–7277.

(15) Bandyopadhyay, P.; Janout, V.; Zhang, L.; Sawko, J. A.; Regen, S. L. *J. Am. Chem. Soc.* **2000**, *122*, 12888–12889.

(16) DiGiorgio, A. F.; Otto, S.; Bandyopadhyay, P.; Regen, S. L. *J. Am. Chem. Soc.* **2000**, *122*, 11029–11030.

(17) Kobuke, Y.; Nagatani, T. *J. Org. Chem.* **2001**, *66*, 5094–5101.

(18) Yoshino, N.; Satake, A.; Kobuke, Y. *Angew. Chem., Int. Ed. Eng.* **2001**, *40*, 457–459.

(19) Sánchez-Quesada, J.; Kim, H. S.; Ghadiri, M. R. *Angew. Chem., Int. Ed. Eng.* **2001**, *40*, 2503–2506.

(20) Kobuke, Y.; Ueda, K.; Sokabe, M. *Chem. Lett.* **1995**, 435–436.

(21) Fyles, T. M.; Loock, D.; Zhou, X. *J. Am. Chem. Soc.* **1998**, *120*, 2997–3003.

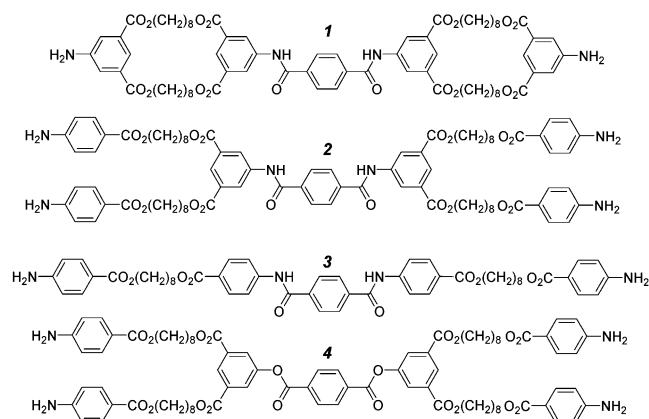
(22) Goto, C.; Yamamura, M.; Satake, A.; Kobuke, Y. *J. Am. Chem. Soc.* **2001**, *123*, 12152–12159.

(23) Schlesinger, P. H.; Ferdani, R.; Liu, J.; Pajewska, J.; Pajewski, R.; Saito, M.; Shabany, H.; Gokel, G. W. *J. Am. Chem. Soc.* **2002**, *124*, 1848–1849.

(24) Fyles, T. M.; Knoy, R.; Müllen, K.; Sieffert, M. *Langmuir* **2001**, *17*, 6669–6674.

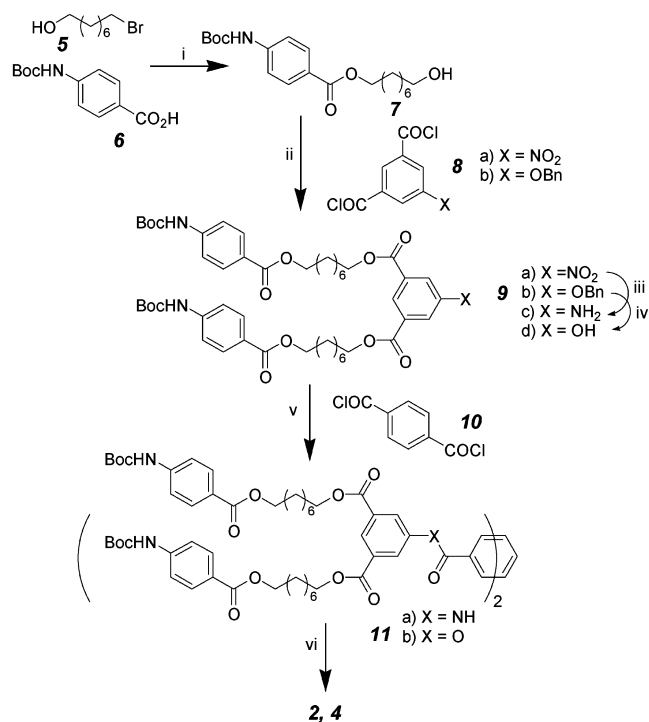
too primitive for development of selective and responsive channels through optimization. An appealing alternative is a “demacrocyclization” strategy demonstrated recently.<sup>25</sup> In this approach, a known active bis-macrocytic bola-amphiphile was conceptually “pruned” to a more easily synthesized acyclic derivative. The acyclic derivative proved to be as active as the parent bis-macrocycle, albeit with diminished cation selectivity. This modest improvement in synthetic efficiency: the bis-macrocycle was available in 0.4% yield after a several month effort, while the acyclic derivative was produced in 50% yield in a few weeks.<sup>25</sup> The acyclic derivative is thus a new lead compound for optimization toward specific performance criteria (selectivity, current rectification).

But is the “demacrocyclization” strategy general? Are there other relatively simple lead compounds that could be prepared simply by “editing” more complex structures? The bis-cyclophane bola-amphiphile compound **1** offers



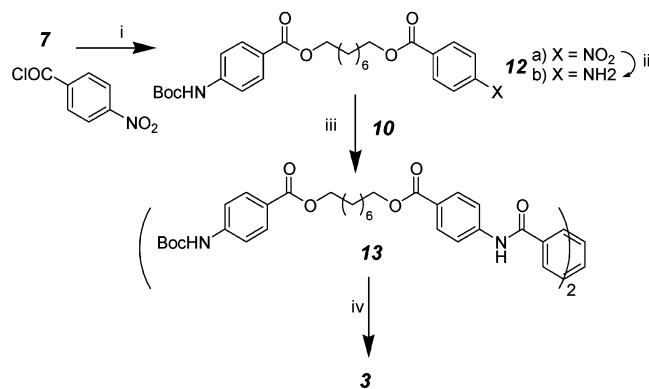
a chance to explore this issue.<sup>26</sup> Despite significant activity in planar bilayer membranes, **1** is destined for obscurity due to a difficult synthesis and extremely poor solubility in all conventional solvents. The cyclophanes of **1** could be opened in a number of ways: compounds **2** and **3** show two possibilities. The branched amphiphile **2** conceptually opens the rings through addition of two new “headgroups”. This construct is topologically similar to the arms of the “bouquet” channels reported by Lehn.<sup>27,28</sup> The alternative linear bola-amphiphile **3** results from removal of one edge of the cyclophane, with some isomeric reorganization. Both **2** and **3** are expected to be more soluble than **1**, but the core terephthalamides might still pose a problem. Accordingly, the ester derivative **4** was considered as well. This report discusses the synthesis of **2–4**, and their activity in vesicle and planar bilayer systems. It directly demonstrates the generality of the “editing” as outlined above, and begins the structure–activity exploration of these new lead compounds through the effect of the amide-to-ester substitution of **2** to **4**.

### SCHEME 1. Synthesis of **2** and **4**<sup>a</sup>



<sup>a</sup> Conditions: (i) Me<sub>4</sub>NOH, DMSO, 50 °C, 14 h, 70%; (ii) Et<sub>3</sub>N, THF, reflux, 12 h, 67–71%; (iii) H<sub>2</sub>, 1% Pt/C, 95% EtOH, 144 h, 89%; (iv) H<sub>2</sub>, 10% Pd/C, EtOH, 14 h, 83%; (v) Et<sub>3</sub>N, THF, reflux, 12 h, 75–84%; (vi) TFA, CH<sub>2</sub>Cl<sub>2</sub>, reflux, 8 h, 79–81%.

### SCHEME 2. Synthesis of **3**<sup>a</sup>



<sup>a</sup> Conditions: (i) Et<sub>3</sub>N, THF, reflux, 12 h, 53%; (ii) H<sub>2</sub>, 5% Pt/C EtOH, 140 h, 88%; (iii) Et<sub>3</sub>N, THF, reflux, 12 h, 90%; (iv) TFA, CH<sub>2</sub>Cl<sub>2</sub>, reflux, 8 h, 82%.

## Results and Discussion

**Synthesis.** The syntheses of **2–4** follow directly from the structures (Schemes 1 and 2). The common precursor **7** was readily prepared from 8-bromooctanol (**5**)<sup>29</sup> and Boc-protected aminobenzoic acid (**6**),<sup>34</sup> via alkylation of

(29) Leonard, L.; Neeland, E.; Onsworth, J.; Sims, R.; Tishler, S.; Weiler, L. *Can. J. Chem.* **1992**, *70*, 1427–1435.

(30) Fyles, T. M.; James, T. D.; Kaye, K. C. *J. Am. Chem. Soc.* **1993**, *115*, 12315–12321.

(31) Fyles, T. M.; Loock, D.; van Straaten-Nijenhuis, W. F.; Zhou, X. *J. Org. Chem.* **1996**, *61*, 8866–8874.

(32) Sakmann, B.; Neher, E. *Single-channel Recording*; Plenum Press: New York, London, 1983.

(33) Valiyaveetil, S.; Müllen, K. *New J. Chem.* **1998**, 89–95.

(25) Fyles, T. M.; Hu, C.; Knoy, R. *Org. Lett.* **2001**.

(26) Cameron, L. M.; Fyles, T. M.; Hu, C. *J. Org. Chem.* **2002**, *67*, 1548–1553.

(27) Julien, L.; Lehn, J.-M. *J. Incl. Phenom. Mol. Recogn. Chem.* **1992**, *12*, 55–74.

(28) Pregel, M. J.; Jullien, L.; Canceill, J.; Lacombe, L.; Lehn, J.-M. *J. Chem. Soc., Perkin Trans. 2* **1995**, 417–426.

the carboxylate salt in DMSO. Subsequent esterification of the isophthaloyl dichlorides **8a,b** gave the tetraesters **9a** and **9b** in approximately 70% yield after chromatography (Scheme 1). The diester **12a** was produced similarly from *p*-nitrobenzoyl chloride (Scheme 2). The protected esters **9a**, **9b**, and **12a** were reduced to compounds **9c**, **9d**, and **12b**, respectively, with H<sub>2</sub> under pressure. The reductions of the nitro compounds were very sluggish and ester degradation was a chronic problem at elevated temperature; thus, it was preferable to proceed slowly at room temperature to give the corresponding amines in good yield. Dimerization of the amines **9c** and **12b** with terephthaloyl dichloride gave the amides **11a** and **13**. As expected, these amides were significantly more soluble than the corresponding protected precursor to **1**. Even so, they were significantly less soluble than the ester **11b**, produced from terephthaloyl chloride and the phenol **9d**. The targets were formed by Boc cleavage with TFA in dichloromethane. The amides **2** and **3** were sufficiently insoluble in dichloromethane to permit trituration to purity. The ester **4** was purified by gel filtration chromatography.

Compounds **2** and **3** were solid powdery materials. Compound **2** dissolved in DMSO with heat, but remained dissolved thereafter. Compound **3** was less soluble than **2**, precipitating from DMSO at concentrations above 20 mM. Compound **4** was a clear glass and dissolved readily in chloroform or methanol. There was no evidence of residual TFA in the carbon NMR spectrum, low-resolution mass spectrum, or the IR spectrum of any of the target compounds. Also, all compounds were slightly basic, as judged by an increase in pH produced by mixing a DMSO solution into unbuffered aqueous solutions. The overall yield for these syntheses from commercially available materials was 13% for **2**, 10% for **3**, and 11% for **4**. The syntheses could be conveniently completed in a few weeks each.

#### Transport Activity in Vesicle Bilayer Membranes.

The transport activity of **2–4** was initially assessed by a pH-stat technique that monitors the collapse of a transmembrane proton gradient in vesicles, typically near neutral inside the vesicle and slightly basic outside.<sup>30,31</sup> This system is a proton–cation antiport; thus, it offers a convenient means to screen the transport selectivity of a range of alkali metal cations. Relative to other active transporters, which were neutral or anionic under the conditions of the experiment, these new compounds were relatively inactive except in acidic solution, presumably where protonation of the amines can occur. The activity was most clearly seen for vesicles that were buffered at pH 3.3 inside and placed in an unbuffered medium held at pH 5 via the pH-stat controller. Under these conditions, compounds **2–4** were capable of provoking a collapse of the transmembrane gradient with release of entrapped protons. Even so, the rate of addition of basic titrant was relatively slow (Figure 1). As noted above, the compounds as isolated are all slightly basic, so the rapid jump following addition of compounds **2** and **3** indicates the combined effect of two competing processes: the efflux of protons from a portion of the vesicles,

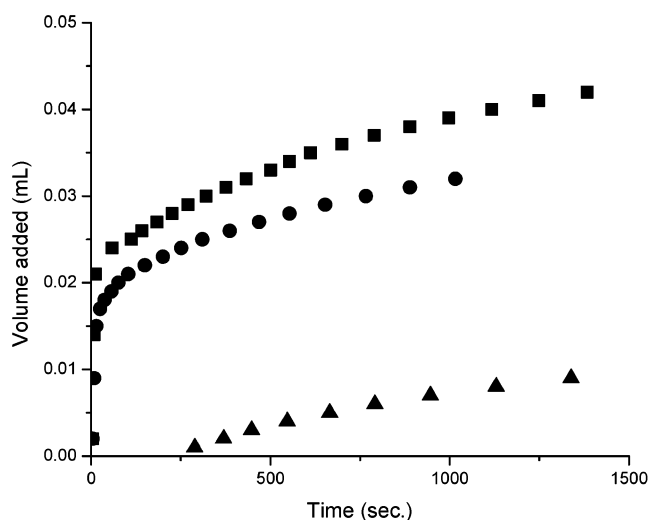


**FIGURE 1.** pH-stat experimental data showing the volume of base added to neutralize proton efflux at pH 5 following treatment of vesicles (PC:PA:cholesterol 8:1:1; 1 mg total lipids) with 0.1  $\mu$ mol of **2** (squares), **3** (circles), or **4** (triangles) (nominal bulk concentration 20  $\mu$ M), as a function of time following compound addition.

some of which are consumed to neutralize the amines of the added transporter. Following this rapid release, there is a period where proton release occurs at a slower rate. The ester **4** does not show the rapid release of acid, thus an “induction” period, where the sample pH is basic relative to the set pH, is needed to establish conditions where a slow release of protons can be measured by the experiment. This confirms that the two processes (release and neutralization) occur independently and there is not just a simple vesicle lysis by the added compound.

The behavior of compounds **2–4** in this vesicle experiment is unlike any system examined previously. In general, the measured transport rates are completely independent of the usual variables of supporting electrolyte (KCl, NaCl, CsCl) and concentration and are largely independent of the amount of compound added. The vertical offset of the curves does depend on the amount of compound added: the higher the initial concentration of **2** or **3**, the larger the initial rapid jump. However, the evolution of the slower process is essentially unchanged. The slow process is apparently only related to the number of intact vesicles available and not to the absolute concentration of compound in the solution, as demonstrated by the addition of fresh vesicle solution (“add back experiment”),<sup>30</sup> which did not accelerate the efflux.

We interpret these results as follows: addition of the compounds initially provokes both a jump to basic pH due to the addition of the amines and a very rapid release of protons from a portion of the vesicles in solution (by **2** or **3**). All three compounds are quite insoluble in water, so precipitation of the injected compound on the surfaces of vesicles is likely in the first few seconds following mixing. The rapid release is absent with **4**, implying some difference in its ability to rapidly form pores. Thereafter, the compounds are slowly redistributed among the remaining intact vesicles. As new vesicles reach a sufficient concentration of compound, a pore opens and the

(34) Mu, F.; Coffing, S. L.; Riese, D. J., III; Geahlen, R. L.; Verdier-Pirand, P.; Hamel, E.; Johnson, J.; Cushman, M. *J. Med. Chem.* **2001**, *44*, 441–447.

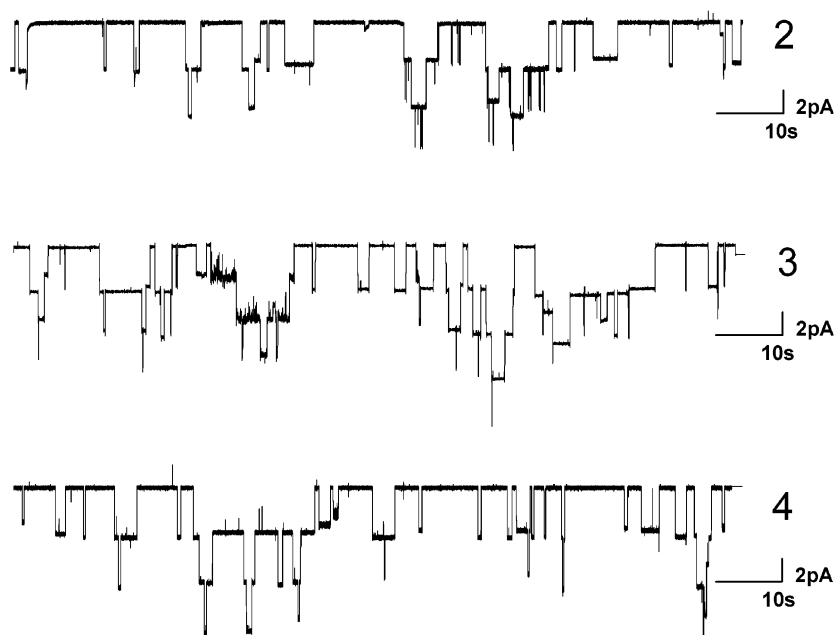


**FIGURE 2.** Typical single-channel behavior observed for compounds **2–4** [–100 mV, diPhyPC, 1 M CsCl; 36 nmol **2**, 33 nmol **3**, 38 nmol **4**; digitally filtered at 100 Hz (**2,4**) or 50 Hz (**3**)].

protons are liberated to be detected by the pH-stat. The slow process does not depend on the concentration of the added compound, so it must be related to some physical transfer between vesicles (by collisions) that is not mediated via a dissolved species. If this interpretation is correct, these compounds exhibit an extreme form of the behavior seen with the most hydrophobic of the crown-ether-based channels investigated previously.<sup>30</sup> The preliminary conclusion from these vesicle studies is that some type of membrane activity is likely for all three compounds, but the nature of the process cannot be studied by this technique.

**Transport Activity in Planar Bilayers.** All three compounds readily form single ion channels in planar bilayer membranes, as assessed by the bilayer clamp technique.<sup>32</sup> Figure 2 illustrates typical current-step behavior for compounds **2–4**. As noted above, the compounds are water insoluble. Activity was generated by injection of 5–10  $\mu\text{L}$  of a DMSO (**2, 4**) or methanol (**3**) solution containing 30–40 nmol of material. The amount directly lost to precipitation (visible) is unknown. Unlike the pH-stat experiment, the compounds were active over the range of pH from 5 to 9; all data presented were obtained at pH 7. Qualitatively, the current records appear closely similar with each compound showing roughly the same magnitude, duration, and frequency of openings under comparable conditions. The majority of openings lie at a single “open” conductance level from the “closed” baseline level, but higher conductance levels are apparent. The proportion of higher conductance levels is related to the concentration of compound added and, for higher concentration experiments, to the length of time from the initial addition. Like other supramolecular transporter systems,<sup>10,13,17</sup> no concentration gives solely the “single channel” opening; thus, the analysis was based on records where the majority of openings (70–80%) were a single transition from the closed state together with multiple openings.

**TABLE 1. Specific Conductance and Permeability Ratios Determined**

	specific conductance (pS)				
	NaCl	CsCl	$P_{\text{Cs}}/P_{\text{Na}}$	$P_{\text{Cs}}/P_{\text{Cl}}$	$P_{\text{Na}}/P_{\text{Cl}}$
<b>2</b>	$10.3 \pm 0.2$	$38.9 \pm 0.4$	$5.2 \pm 0.8$	$7.2 \pm 1.0$	$2.1 \pm 0.9$
<b>3</b>	$10.4 \pm 1.0$	$38.1 \pm 0.9$	$5.6 \pm 1.0$	$7.3 \pm 0.9$	$5.7 \pm 0.8$
<b>4</b>	$10.2 \pm 1.0$	$39.3 \pm 0.9$	$4.7 \pm 1.0$	$7.5 \pm 0.9$	$3.1 \pm 0.5$

The occurrence of multiple levels was examined through histograms of the frequencies of observed conductance. The histogram shown in Figure 3a for compound **4** (derived from the data of Figure 2) is typical in that it shows a regular progression of conductance levels that may be analyzed as a series of Gaussian distributions about a series of means. As previously, this is interpreted as multiple copies of a single type of channel; thus, the value of the regular spacing is taken as the conductance of the channel formed in each case (–3.3 pA in Figure 3a).<sup>31</sup> The conductance of each channel was assessed for symmetrical concentrations of NaCl and CsCl electrolytes over a range of applied transmembrane potentials. Under these conditions, the current as a function of potential gave a linear relationship passing through the origin for all three compounds. This Ohmic behavior implies that compounds **2–4** act as simple resistors to ionic conductance in the membrane. Table 1 gives the specific conductance values determined: all three compounds exhibit cesium selectivity, but there are no differences between the compounds.

A close inspection of Figure 2 shows several examples of open states that do not fall within the regular progression expected but appear to have lower conductance. This behavior is general for the three compounds. Figure 4 shows a number of examples within a restricted time window found in an experiment using compound **4** with CsCl electrolyte. This record includes a clear example in which two different low-conductance states are seen to

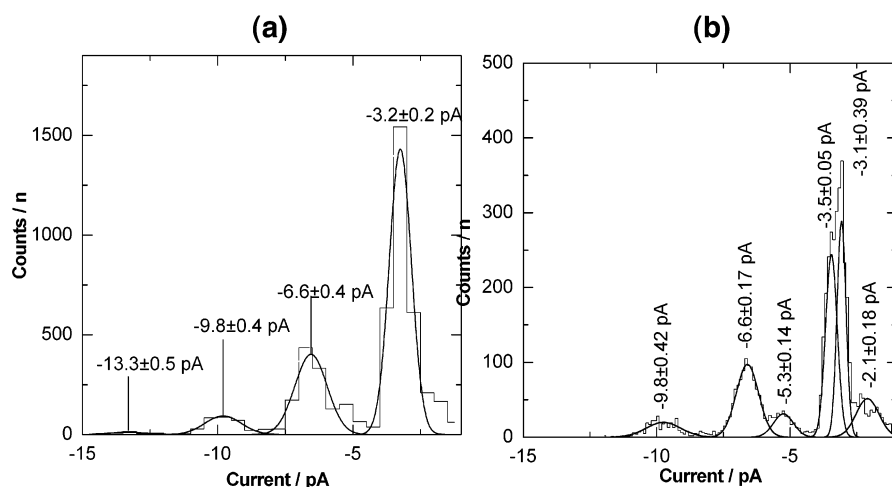


**FIGURE 3.** (a) Histogram of conductance levels for **4** (data of Figure 2, bin width 0.5 pA). (b) The same data with a bin width of 0.1 pA.

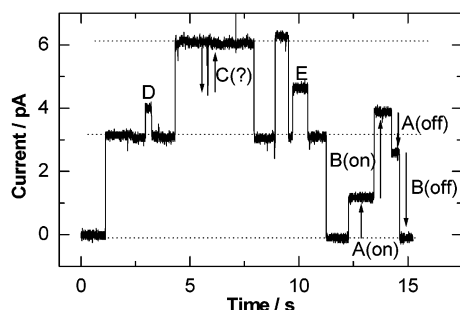


**FIGURE 4.** Portion of the single-channel record of **4** (+80 mV, diPhyPC, 1 M CsCl, 36 nmol) showing examples of lower conductance channel events (A–E).

open and close independently (A/B open/closed marked). The sublevel states might also be produced from the dominant open states and a possible example of this behavior is also marked in Figure 4 (C closed/open). These sublevels are readily found by visual inspection, but they are rare and therefore of limited statistical significance. They are not evident in any of the histograms produced at the 0.5 pA bin size, as was illustrated in Figure 3a. A “rebinning” of the data set used to create Figure 3a was done at 0.1 pA bin width and is shown as Figure 3b. Immediately obvious in this presentation is the emergence of sublevel populations. Each population was fit to a Gaussian distribution to account for thermal variation within each conducting state. The result shows that the dominant open states give rather narrow distributions compared to the minor sublevel states. This “rebinning” procedure reveals some of the levels that are obvious in visual inspection, but it does not make them any more significant in the overall behavior of the system. The system behaves as a dominant state, usually a single opening from the baseline but also occurring as multiple copies, together with a variety of minor openings of lower conductance.

The ionic selectivity of the dominant opening was further determined from the current–potential relationships derived for various salt gradients across the bilayer membrane. The Goldman–Hodgkin–Katz equation<sup>32</sup>

$$V_{\text{rev}} = \frac{RT}{F} \ln \left( \frac{P_{\text{Na}}\gamma_{\text{Na}}[\text{Na}^+]_{\text{trans}} + P_{\text{Cs}}\gamma_{\text{Cs}}[\text{Cs}^+]_{\text{trans}} + P_{\text{Cl}}\gamma_{\text{Cl}}[\text{Cl}^-]_{\text{cis}}}{P_{\text{Na}}\gamma_{\text{Na}}[\text{Na}^+]_{\text{cis}} + P_{\text{Cs}}\gamma_{\text{Cs}}[\text{Cs}^+]_{\text{cis}} + P_{\text{Cl}}\gamma_{\text{Cl}}[\text{Cl}^-]_{\text{trans}}} \right) \quad (1)$$

relates the “reversal potential” ( $V_{\text{rev}}$ , defined as the point of zero net ionic current) to individual ionic permeabilities ( $P_X$ , the permeability of either cation or anion X) and to the activities of the individual ions in the contacting aqueous solutions ( $\gamma_X$ ). The subscripts cis and trans refer to the two sides of the bilayer chamber with the convention that the trans side is defined as virtual ground. The constants  $R$ ,  $T$ , and  $F$  are the standard gas constant, temperature, and Faraday constant, respectively. Under conditions of differing concentrations of a single salt across the bilayer, the ratio of cation/anion permeability can be calculated based on the assumption that  $P_{\text{anion}} < P_{\text{cation}}$ . Alternatively, under conditions of equivalent concentrations of different salts (1 M CsCl cis:1 M NaCl trans), a permeability ratio can be calculated for the two cations. Figure 5 shows typical results obtained in the derivation of ionic permeability ratios. Each point is the mean value determined from an all-points histogram calculated at a bin width of 0.5 pA (as in Figure 3a). A best-fit binomial was used in each case to derive the point of zero net current,  $V_{\text{rev}}$ , denoted by the arrows in Figure 5. The results of these ion selectivity experiments are also summarized in Table 1. The observed ion selectivity directly follows the order of the single-ion hydration energies ( $\text{Cs}^+ < \text{Na}^+ < \text{Cl}^-$ ), as found with other bola-amphiphile channels.<sup>31</sup>

Further characterization was achieved by lifetime measurements. For this analysis a data set with predominantly single-level openings from the baseline was acquired from an experiment in which the added compound was incorporated at an apparently lower concentration. The lower concentration resulted in less frequent openings, so data sets of 45–80 min duration were obtained to produce sufficient numbers of openings. A list of opening durations was produced and plotted as a histogram of the number of channels open within a given time window. A stochastic deactivation process, for

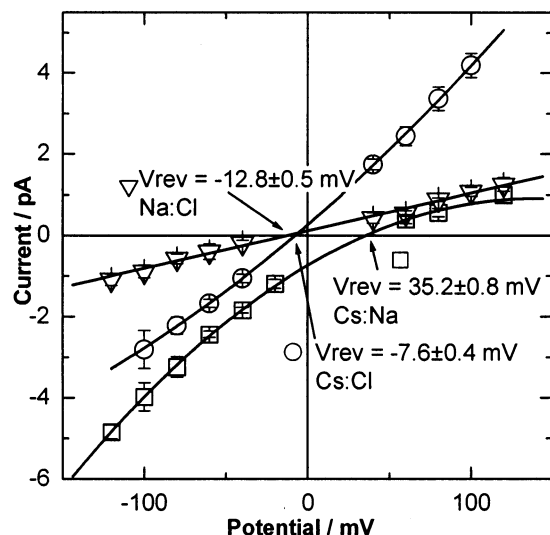


**FIGURE 5.** Current–voltage relationships for 32 nmol **4** under asymmetric electrolyte conditions, where arrows indicate points of zero net current,  $V_{\text{rev}}$ : 1 M CsCl:0.1 M CsCl (circles); 1 M NaCl:0.1 M NaCl (triangles); 1 M CsCl:1 M NaCl (squares).

**TABLE 2.** Lifetime Data

	$A_1/A_T^a$	$\tau_1$ (ms)	$A_2/A_T^a$	$\tau_2$ (ms)
<b>2</b>	1.0	$277 \pm 5$		
<b>3</b>	0.96	$64 \pm 1$	0.04	$682 \pm 31$
<b>4</b>	0.97	$117 \pm 6$	0.03	$842 \pm 157$

<sup>a</sup>  $A_i/A_T$  gives the proportional weighting of the biexponential fit.

example, as a result of thermal motions within the bilayer, would result in an exponential decrease in the numbers of channels open as a function of time.<sup>32</sup> The decrease can be fit to an exponential function to yield a characteristic lifetime ( $\tau$ ) of the channels.

The data for compound **2** could be adequately fit to a single exponential, but compounds **3** and **4** required analysis as a sum of two exponentials to account for a small proportion of long-lived openings. The single channel open durations were derived automatically and may include some unrecognized multiple openings of long duration that would contribute to very long-lived openings. The derived values are summarized in Table 2. The shorter-lived and dominant component of compounds **3** and **4** can be directly compared with the single value obtained for **2**. This shows a 4-fold increase in lifetime along the series **3** < **4** < **2**. That **3** has the shortest lifetime is consistent with the lower molecular weight of this compound making it more susceptible to thermally induced collisions within the bilayer. The longer lifetime of **2** relative to **4** would be consistent with a possible stabilization via self-hydrogen-bonding of the amides in **2**, which is not possible with **4**. However, this appealing interpretation must be tempered by the observation that **2** does not produce the very long-lived channels found with **3** and **4**.

The lifetime analysis treats all openings independently of the conductance of the opening. Given the existence of a population of sublevel openings, this begs the question of the lifetime of these minor levels relative to the dominant openings. Figure 6 shows a two-dimen-

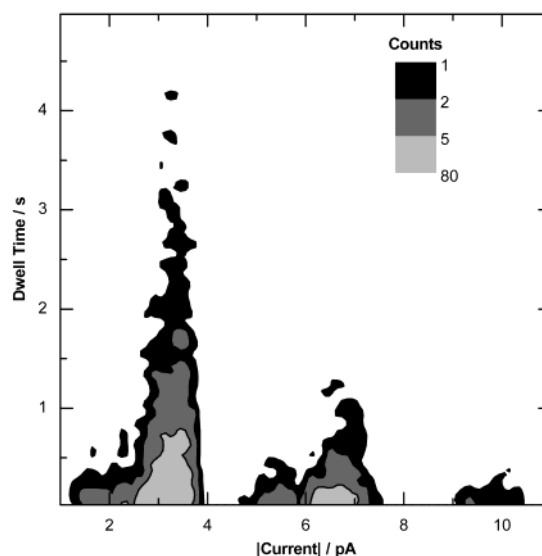


**FIGURE 6.** Two-dimensional histogram plot of channel opening time and channel current for **4** (100 mV, diPhyPC, 1 M CsCl, 38 nmol).

sional histogram contour plot of the duration of opening as a function of the opening conductance for the experiment of Figure 3. If each conductance level within a unitary opening had the same lifetime, then this plot should produce a symmetrical distribution along the conductance axis. As illustrated in Figure 6, the distributions about the conductance peaks are asymmetrical, with a skew toward longer lived states of higher conductance. This contour plot provides direct evidence that sublevel opening events are both less frequent and shorter lived. This conclusion is general for all three compounds.

## Conclusion

The question posed in the Introduction—is the “de-macrocytization strategy” general?—has been clearly affirmed. Not only are compounds **2–4** simpler to make and handle than compound **1**, all three readily form channels in bilayer membranes. However, the close similarity between the activities of the three compounds is surprising, given that there are considerable structural differences between the structures of compounds **2** and **4** and compound **3**. The only significant experimental differences detected among the three compounds are in the channel lifetimes and in the puzzling behaviors in the pH-stat experiment. As noted above, the lifetime differences might be rationalized through structural arguments, but these are tenuous.

The nature of the active structure(s) remains in the realm of speculation. By analogy with other bola-amphiphile channels,<sup>31</sup> active aggregates (dimers, trimers) may be involved, but the important stoichiometric support for this assumption, derived previously from vesicle experiments, is not available for these three compounds, nor is it obvious that these flexible structures must span the membrane. Figure 7 presents some of the possibilities relative to a lipid tail-to-tail dimer to indicate the membrane. The membrane-spanning orientation **A** is a compatible length to span the bilayer core as assessed

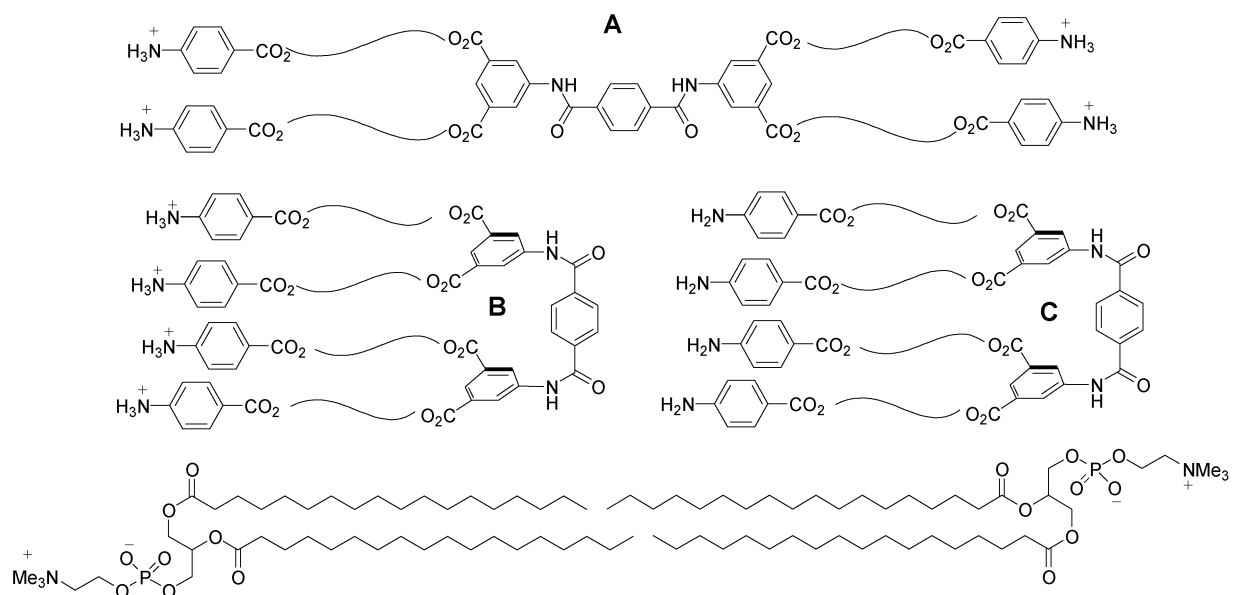


**FIGURE 7.** Possible orientations in a bilayer membrane of the bola-amphiphiles prepared.

from models. This orientation places the amides near the bilayer midplane, and if active dimer or other aggregates are involved, in proximity to other amides for self-hydrogen-bonding. As noted above, the similar activities of **2** and **4** suggest that this type of self-recognition is not likely to be significant. Alternatively, the carbonyls can act as hydrogen-bond acceptors for a water pool at the bilayer midplane. The bent conformations **B/C** are possible alternatives, either with the aniline groups at the aqueous interface (**B**) or buried in the bilayer (**C**). In acidic pH the anilines would be partly or fully protonated; conformation **C** would be unfavorable, except if the anilines were neutral. Conformations **B** and **C** appear to require *cis*-amides, as other bending possibilities explored with modeling did not lead to compact structures. Of these three choices, the membrane spanning state of the bilayer, having a long axis and defined polarity for interaction with the surface regions. Further progress toward a mechanism will require other derivatives to explore the structure–activity questions more fully.

A key feature of these compounds is the existence of sublevels. These are both less probable and shorter lived than the dominant openings, but nonetheless, they can open and close as discrete entities. The relative breadth of the thermal distributions for these levels indicates that they are less tightly defined than the structures that produce the dominant openings. If membrane-spanning structures were involved, then the sublevels could arise as a result of conformational isomers (amide rotations) of the components or as a result of different aggregation geometries or aggregation numbers. Whatever the active structures might be, it is unlikely that self-hydrogen-bonding of the terephthalamides plays a significant role. The amide-to-ester change of **2** to **4** results in channel behaviors that are virtually indistinguishable. We are confident in the conclusion that this particular region of the structure is unrelated to the overall activity produced.

## Experimental Section

**8-Bromoocetan-1-ol (5)** was prepared as described by Weiler.<sup>29</sup> **5-Benzyloxyisophthaloyl chloride (8b)** was prepared from the known acid<sup>33</sup> by action of thionyl chloride.

**4-tert-Butoxycarbonylamidobenzoic Acid (6).**<sup>34</sup> 4-Aminobenzoic acid (6.40, 46.7 mmol) was dissolved in 60:40 water:methanol saturated with sodium carbonate and heated to 40 °C. Di-*tert*-butyl carbonate (10.24 g, 46.9 mmol) was added dropwise. The solution was allowed to stir for 14 h. The pH was adjusted to 3 with acetic acid and the precipitate was removed by filtration. Vacuum drying gave **6** (9.74 g, 88%). <sup>1</sup>H NMR, acetone-*d*<sub>6</sub>: 8.78 (s, 1H), 7.98 (d, 8.8 Hz, 2H), 7.68 (d, 8.8 Hz, 2H), 1.42 (s, 9H). <sup>13</sup>C NMR, acetone-*d*<sub>6</sub>: 167.4, 153.4, 145.0, 131.6, 124.9, 118.1, 80.6, 28.4.

**(8-Hydroxyoctyl) 4-tert-Butoxycarbonylamidobenzoate (7).** Tetramethylammonium hydroxide (2.84, 15.7 mmol) was dissolved in DMSO (100 mL). Compound **6** (3.28 g, 14.6 mmol) and sodium iodide (0.23 g, 1.5 mmol) dissolved in DMSO were added and the solution was heated at 50 °C under N<sub>2</sub>. Compound **5** (3.28 g, 15.7 mmol) was added dropwise. The solution was stirred for 14 h. Deionized water (900 mL) was then added and the precipitate was filtered and dried under vacuum. The crude product was purified by column chromatography on silica using a 3:7 hexane:ether eluent to give **7** (3.74 g, 70%). <sup>1</sup>H NMR acetone-*d*<sub>6</sub>: 8.78 (s, 1H), 7.94 (d, 8.7 Hz, 2H), 7.66 (d, 8.7 Hz, 2H), 4.25 (t, 7.5 Hz, 2H), 3.50 (t, 7.5 Hz, 2H), 1.8–1.2 (br s, 21H). <sup>13</sup>C NMR, acetone-*d*<sub>6</sub>: 166.4, 153.4, 145.0, 131.2, 124.9, 118.1, 80.6, 65.2, 62.4, 33.7, 28.4, 26.7, 26.6. MS (EI) exact mass calculated for (C<sub>20</sub>H<sub>31</sub>NO<sub>5</sub>)<sup>+</sup> 365.2202, found 365.2193.

**Bis[8-(4-tert-butoxycarbonylamidobenzoyl)octyl] 5-Nitroisophthalate (9a).** The commercially available acid chloride **8a** (1.25, 5.04 mmol) and triethylamine (2.04 g, 20.16) were dissolved in dry THF (50 mL). Compound **7** (3.68 g, 10.1 mmol) dissolved dry THF (100 mL) was added and the mixture heated to reflux at 90 °C for 14 h. The crude product was purified by column chromatography on silica using 3:7 hexane:ether eluent to give **9a** (3.24 g, 71%). <sup>1</sup>H NMR, CDCl<sub>3</sub>: 8.99 (s, 2H), 8.93 (s, 1H), 7.94 (d, 8.8 Hz, 4H), 7.42 (d, 8.8 Hz, 4H), 6.81 (s, 2H), 4.38 (t, 7.5 Hz, 4H), 4.29 (t, 7.5 Hz, 4H), 1.8–1.2 (m, 42H). <sup>13</sup>C NMR, CDCl<sub>3</sub>: 166.3, 163.8, 152.3, 148.4, 142.8, 135.8, 132.8, 130.9, 128.0, 124.5, 117.3, 81.1, 66.4, 64.8, 29.1, 28.7, 28.5, 28.3, 25.9, 25.8. MS (EI) exact mass calculated for (C<sub>48</sub>H<sub>64</sub>N<sub>3</sub>O<sub>14</sub>)<sup>+</sup> 905.4310, found 905.4321.

**Bis[8-(4-*tert*-butoxycarbonylamidobenzoyl)octyl] 5-Benzoyloxyisophthalate (9b).** Compound **8b** (0.96, 3.1 mmol) and triethylamine (2.50 g, 24.7 mmol) were dissolved in dry THF (50 mL). Compound **7** (2.08 g, 5.69 mmol) dissolved in dry THF (100 mL) was added and the mixture was heated to reflux at 90 °C for 18 h. The crude product was purified by column chromatography on silica using a 3:5:2 chloroform:ether:hexane eluent to yield **9b** (2.01 g, 67%). <sup>1</sup>H NMR, CDCl<sub>3</sub>: 8.29 (s, 1H), 7.97 (d, 8.4 Hz, 4H), 7.81 (s, 2H), 7.30 (m, 9H), 6.85 (s, 2H), 5.14 (s, 2H), 4.25 (m, 8H), 1.8–1.2 (m, 42H). <sup>13</sup>C NMR, CDCl<sub>3</sub>: 166.3, 165.7, 158.7, 152.2, 142.7, 136.1, 132.2, 130.8, 128.7, 128.3, 127.6, 124.7, 123.2, 120.0, 117.4, 81.1, 70.5, 65.5, 64.8, 29.1, 28.7, 28.6, 28.3, 26.0, 25.9.

**Bis[8-(4-*tert*-butoxycarbonylamidobenzoyl)octyl] 5-Aminoisophthalate (9c).** Compound **9a** (1.2 g, 1.32 mmol) was dissolved in 100 mL of 95% ethanol, and 1.8 g of 1% Pt/C was added. The solution was placed under 50 psi of hydrogen for 144 h. The catalyst was removed by filtration, the solvent was removed by evaporation, and the crude product was purified by column chromatography on silica using an 80:20:1 toluene:ethyl acetate:pyridine eluent to give **9c** (1.03 g, 89%). <sup>1</sup>H NMR CDCl<sub>3</sub>: 8.01 (s, 1H), 7.94 (d, 8.4 Hz, 4H), 7.47 (s, 2H), 7.42 (d, 8.4 Hz, 4H), 7.18 (s, 2H), 4.25 (m, 8H), 4.02 (s, 2H), 1.8–1.0 (m, 42H). <sup>13</sup>C NMR, CDCl<sub>3</sub>: 166.4, 166.1, 152.3, 146.8, 142.8, 131.8, 130.8, 124.6, 120.5, 119.6, 117.4, 81.0, 65.3, 64.8, 29.1, 28.7, 28.6, 28.3, 25.9, 25.9.

**Bis[8-(4-*tert*-butoxycarbonylamidobenzoyl)octyl] 5-Hydroxyisophthalate (9d).** Compound **9b** (0.88 g, 0.900 mmol) was dissolved in 50 mL of 100% ethanol, and 1.00 g of 10% Pd/C was added. The solution was stirred under 60 psi of hydrogen for 14 h. The catalyst was removed by filtration, the solvent removed by evaporation, and the crude product was purified by column chromatography on silica using a 5:4:1:0.1 chloroform:ether:hexane:pyridine eluent to yield **9d** (0.66 g, 83%). <sup>1</sup>H NMR, CDCl<sub>3</sub>: 8.22 (s, 1H), 7.94 (d, 8.5 Hz, 4H), 7.73 (s, 2H), 7.42 (d, 8.5 Hz, 4H), 6.84 (s, 2H), 4.30 (m, 8H), 1.8–1.2 (m, 42H). <sup>13</sup>C NMR, CDCl<sub>3</sub>: 166.5, 166.0, 157.4, 152.4, 142.9, 132.0, 130.8, 124.5, 122.0, 120.9, 117.4, 81.1, 65.3, 34.9, 28.1, 28.7, 28.6, 28.3, 25.9, 25.9. LSIMS (mNBA) exact mass calculated for (C<sub>48</sub>H<sub>65</sub>N<sub>2</sub>O<sub>13</sub>)<sup>+</sup> 877.4487, found 877.4487.

**N,N'-Bis(3,5-bis[8-(4-*tert*-butoxycarbonylamidobenzoyl)octyl]carboxyphenyl)terephthalamide (11a).** Terephthaloyl dichloride (**10**) (0.023 g, 0.113 mmol) was dissolved in dry THF (10 mL), and triethylamine (0.20 g, 1.98 mmol) was added. Compound **9c** (0.2 g, 0.228 mmol) dissolved in dry THF (25 mL) was added and the solution stirred at 90 °C for 12 h. The crude product was purified by column chromatography on silica using a 20:80:1 ethyl acetate:toluene:acetic acid eluent to give **11a** (0.18 g, 84%). <sup>1</sup>H NMR, CDCl<sub>3</sub>: 9.09 (s, 2H), 8.57 (s, 4H), 8.42 (s, 2H), 7.90 (m, 12H), 7.41 (d, 8.4 Hz, 8H), 7.02 (s, 2H), 4.25 (m, 16H), 1.8–1.2 (m, 84H). <sup>13</sup>C NMR, CDCl<sub>3</sub>: 166.5, 165.6, 165.4, 152.4, 142.9, 138.6, 137.5, 131.7, 130.7, 127.7, 126.6, 125.6, 124.5, 117.4, 81.0, 65.7, 64.9, 29.1, 28.6, 28.5, 28.2, 25.9. LSIMS (mNBA) exact mass calculated for (C<sub>84</sub>H<sub>101</sub>N<sub>6</sub>O<sub>18</sub>)<sup>+</sup> (M – 4Boc) 1481.7172, found 1481.7164.

**Bis(3,5-bis[8-(4-*tert*-butoxycarbonylamidobenzoyl)octyl]carboxyphenyl)terephthalate (11b).** Terephthaloyl dichloride (**10**) (0.067 g, 0.330 mmol) was dissolved in dry THF (10 mL), and triethylamine (0.30 g, 3.0 mmol) was added. Compound **9d** (0.60 g, 0.684 mmol) dissolved in dry THF (25 mL) was added and the solution stirred at 90 °C for 12 h. The crude product was purified by column chromatography on silica using a 5:4:1:0.1 chloroform:ether:hexane eluent, to yield **11b** (0.47 g, 75%). <sup>1</sup>H NMR, CDCl<sub>3</sub>: 8.58 (s, 2H), 8.34 (s, 4H), 8.04 (s, 4H), 7.91 (d, 8.4 Hz, 8H), 7.38 (d, 8.4 Hz, 8H), 6.72 (s, 4H), 4.31 (t, 7.5 Hz, 8H), 4.22 (t, 7.5 Hz, 8H), 1.8–1.2 (m, 84H). <sup>13</sup>C NMR, CDCl<sub>3</sub>: 166.3, 164.9, 163.8, 152.2, 150.6, 142.6, 133.5, 132.6, 130.8, 130.5, 128.3, 127.0, 124.7, 117.3, 81.1, 65.8, 64.8, 29.1, 28.7, 28.6, 28.3, 25.9.

**[8-(4-*tert*-Butoxycarbonylamidobenzoyl)octyl] 4-Nitrobenzoate (12a).** 4-Nitrobenzoyl chloride (1.5, 8.08 mmol) and triethylamine (3.32 g, 32.8 mmol) were dissolved in dry

THF (10 mL). Compound **7** (3.00 g, 8.21 mmol) dissolved in dry THF (100 mL) was added and the mixture heated to reflux at 90 °C for 14 h. The crude product was purified by column chromatography on silica using 3:4:3 chloroform:ether:hexane eluent to give **12a** (2.20 g, 53%). <sup>1</sup>H NMR, CDCl<sub>3</sub>: 8.23 (d, 8.4 Hz, 2H), 8.18 (d, 8.4 Hz, 2H), 7.94 (d, 8.4 Hz, 2H), 7.38 (d, 8.4 Hz, 2H), 6.92 (s, 1H), 4.32 (t, 7.4 Hz, 2H), 4.25 (t, 7.4 Hz, 2H), 1.8–1.2 (m, 21H). <sup>13</sup>C NMR, CDCl<sub>3</sub>: 166.3, 164.7, 152.3, 150.5, 142.8, 135.9, 130.8, 130.6, 124.6, 123.5, 117.4, 81.0, 66.0, 64.8, 29.4, 28.7, 28.6, 28.2, 25.9, 25.9. LSIMS (mNBA) exact mass calculated for (C<sub>27</sub>H<sub>34</sub>N<sub>2</sub>O<sub>8</sub>)<sup>+</sup> 514.2314, found 514.2315.

**[8-(4-*tert*-Butoxycarbonylamidobenzoyl)octyl] 4-Aminobenzoate (12b).** Compound **12a** (2.1 g, 4.08 mmol) was dissolved in 100 mL of 95% ethanol and 0.5 g of 5% Pt/C was added. The solution was stirred under 50 psi of hydrogen for 144 h. The catalyst was removed by filtration, the solvent was removed by evaporation, and the crude product was purified by column chromatography on silica using an 5:4:1 chloroform:ether:hexane eluent to yield **12b** (1.74 g, 88%). <sup>1</sup>H NMR, CDCl<sub>3</sub>: 7.94 (d, 8.6 Hz, 2H), 7.84 (d, 8.4 Hz, 2H), 7.42 (d, 8.4 Hz, 2H), 6.67 (s, 1H), 6.61 (d, 8.6 Hz, 2H), 4.25 (m, 4H), 4.03 (s, 2H), 1.8–1.2 (m, 21H). <sup>13</sup>C NMR, CDCl<sub>3</sub>: 166.7, 166.3, 152.7, 150.7, 142.6, 131.5, 130.8, 124.8, 120.2, 117.3, 113.8, 81.2, 64.9, 64.4, 29.2, 28.8, 28.7, 28.3, 26.0, 25.9. LSIMS (mNBA) exact mass calculated for (C<sub>27</sub>H<sub>36</sub>N<sub>2</sub>O<sub>6</sub>)<sup>+</sup> 484.2573, found 484.2575.

**N,N'-Bis(4-[8-(4-*tert*-butoxycarbonylamidobenzoyl)octyl]carboxyphenyl)terephthalamide (13).** Terephthaloyl dichloride (0.15 g, 0.74 mmol) was dissolved in dry THF (10 mL), and triethylamine (0.62 g, 6.1 mmol) was added. Compound **12b** (0.712 g, 1.46 mmol) dissolved in dry THF (25 mL) was added and the solution was stirred at 90 °C for 14 h. The crude product was purified by column chromatography on silica using a 20:80:1 ethyl acetate:toluene:acetic acid eluent to yield **13** (0.73 g, 90%). <sup>1</sup>H NMR, DMSO-*d*<sub>6</sub>: 10.70 (s, 2H), 9.75 (s, 2H), 8.11 (s, 4H), 7.98 (s, 8H), 7.88 (d, 8.5 Hz, 4H), 7.61 (d, 8.5 Hz, 4H), 4.25 (m, 8H), 1.8–1.2 (m, 42H). <sup>13</sup>C NMR, DMSO-*d*<sub>6</sub>: 165.4, 165.2, 152.5, 144.1, 143.4, 137.3, 130.2, 130.1, 127.9, 124.8, 123.0, 119.7, 117.3, 79.7, 64.5, 64.2, 28.6, 28.2, 28.0, 25.4. LSIMS (mNBA) exact mass calculated for (C<sub>62</sub>H<sub>75</sub>N<sub>4</sub>O<sub>14</sub>)<sup>+</sup> 1099.5280, found 1099.5274.

**N,N'-Bis(3,5-bis[8-(4-amidobenzoyl)octyl]carboxyphenyl)terephthalamide (2).** Compound **11a** (0.10 g, 53 μmol) was dissolved in dichloromethane (25 mL), and trifluoroacetic acid (0.26 g, 0.20 mmol) was added. The mixture was stirred at 60 °C for 14 h. The solution was decanted and the solid was washed with chloroform and dried under vacuum to yield **2** (0.062 g, 79%). <sup>1</sup>H NMR, DMSO-*d*<sub>6</sub>: 10.88 (s, 2H), 8.75 (s, 4H), 8.23 (s, 2H), 8.16 (s, 4H), 7.72 (d, 8.6 Hz, 8H), 6.79 (d, 8.6 Hz, 8H), 4.70 (s, broad, exch D<sub>2</sub>O), 4.35 (t, 7.4 Hz, 8H), 4.18 (t, 7.5 Hz, 8H), 1.8–1.2 (m, 48H). <sup>13</sup>C NMR, DMSO-*d*<sub>6</sub>: 165.9, 165.2, 164.8, 153.4, 140.0, 137.1, 131.0, 130.9, 127.9, 124.7, 116.0, 112.6, 65.2, 63.5, 28.6, 28.6, 28.3, 28.1, 25.5. LSIMS (mNBA) exact mass calculated for (C<sub>84</sub>H<sub>101</sub>N<sub>6</sub>O<sub>18</sub>)<sup>+</sup> 1481.7172, found 1481.7181.

**N,N'-Bis(4-[8-(4-amidobenzoyl)octyl]carboxyphenyl)terephthalamide (3).** Compound **13** (0.70 g, 0.64 mmol) was dissolved in dichloromethane (25 mL), and trifluoroacetic acid (0.66 g, 5.8 mmol) was added. The mixture was stirred at 60 °C for 14 h. The solution was decanted and the solid was washed with chloroform and dried under vacuum to give **3** (0.46 g, 80%). <sup>1</sup>H NMR, DMSO-*d*<sub>6</sub>: 10.71 (s, 2H), 8.13 (s, 4H), 8.00 (s, 8H), 7.63 (d, 8.5 Hz, 4H), 6.57 (d, 8.5 Hz, 4H), 5.94 (br, 4H), 4.25 (t, 7.5 Hz, 4H), 4.17 (t, 7.5 Hz, 4H), 1.8–1.2 (m, 24H). <sup>13</sup>C NMR, DMSO-*d*<sub>6</sub>: 165.9, 165.4, 165.2, 153.4, 143.4, 137.3, 131.0, 130.1, 127.9, 124.9, 119.7, 116.1, 112.6, 64.4, 63.5, 28.6, 28.4, 28.2, 25.5. LSIMS (mNBA) exact mass calculated for (C<sub>52</sub>H<sub>59</sub>N<sub>4</sub>O<sub>10</sub>)<sup>+</sup> 899.4231, found 899.4178.

**Bis(3,5-bis[8-(4-aminobenzoyl)octyl]carboxyphenyl)terephthalate (4).** Compound **11a** (0.052 g, 41 μmol) was dissolved in dichloromethane (10 mL), and trifluoroacetic acid (0.2 g, 5.8 mmol) was added. The mixture was stirred at 60



°C for 14 h. The mixture was then washed three times with a saturated solution of sodium bicarbonate and purified by gel filtration on bio beads SX-3 with dichloromethane as eluent to give **4** (0.033 g, 82%). <sup>1</sup>H NMR, CDCl<sub>3</sub>: 8.63 (s, 2H), 8.36 (s, 4H), 8.10 (s, 4H), 7.81 (d, 8.4 Hz, 8H), 6.60 (d, 8.4 Hz, 8H), 4.36 (t, 7.5 Hz, 8H), 4.22 (t, 7.5 Hz, 8H), 4.08 (s, 2H), 1.8–1.2 (m, 48H). <sup>13</sup>C NMR, CDCl<sub>3</sub>: 166.7, 164.9, 163.9, 150.8, 150.3, 133.5, 132.6, 131.5, 130.5, 128.4, 127.0, 117.0, 113.8, 65.9, 64.4, 29.1, 28.8, 28.6, 26.0, 25.9. LSIMS (mNBA) exact mass calculated for (C<sub>84</sub>H<sub>99</sub>N<sub>4</sub>O<sub>20</sub>)<sup>+</sup> 1483.6853, found 1483.6845.

**Vesicle Experiments.** Vesicles were prepared from mixed lipids [egg phosphatidyl choline (PC), phosphatidic acid (PA), and cholesterol (8:1:1 mole ratio; 16:2:1 weight ratio)] by the sonication–reverse evaporation method used previously with a different set of internal and external buffer solutions and set pH.<sup>24,31</sup> The internal buffer solution (pH-stat = 5) was 0.2 M citric acid, 0.054 M D-mannitol, with the pH adjusted to 3.3 with choline hydroxide, and the external solution (pH-stat = 5) was 0.11 M choline sulfate, 0.093 M D-mannitol, with the pH adjusted to 4.5 with sulfuric acid. A film of mixed lipids (50 mg, from chloroform stock by evaporation under vacuum overnight) was dissolved in ether (6 mL) and the internal buffer solution (2 mL) was added. Sonication of the lipid/ether/buffer solution (Heat Systems W385 Ultrasonic, 13 mm insertion probe, 50% power, 50% duty cycle, 30 pulses) mixed the biphasic solution to homogeneity. The ether was removed by slow rotary evaporation, the external solution was added (3 mL), and rotary evaporation was continued for another 30 min at reduced pressure (ca. 500 mmHg). Vesicles were sized using a LiposoFast membrane apparatus (Avestin, 0.4 μm pore size) and the resultant solution was purified by a gel filtration column (Sephadex G-25 column equilibrated with external solution cooled to below 10 °C). A typical preparation contained a bimodal population of vesicles (Nicomp dynamic light scattering; 80–85% 230 nm diameter, 20–15% 80 nm diameter) at a lipid concentration of 10–12 mg/mL. Vesicles were used within 48 h of preparation.

**pH-stat Titration.** A sample of external solution (5 mL) in a thermostated titration cell (25 °C) was brought to the desired set pH via addition of choline hydroxide titrant (5.23 mM; 0.335 M mannitol) under the control of an automatic titrimer (Mettler DL21 interfaced to Excel via a serial port). Vesicle dispersion (100 μL, 1 mg of lipids) was added to the cell, followed by FCCP [carbonyl cyanide 4-(trifluoromethoxy)-phenylhydrozone], 25 μL of a 10 mM solution in methanol and the desired alkali metal sulfate (50 μL of a 1 M solution). The titrimer was allowed to adjust the pH to the set value throughout this sequence of additions. Variable amounts of transporter were added (time = 0) and the titrimer responded to the proton efflux. Once the system had reached an apparent plateau (500–1000 s), Triton X-100 (200 μL of a 0.1 wt % solution) was added to the cell to lyse any remaining vesicles.

**Bilayer Clamp Experiments.** A model BC-525A bilayer clamp (Warner Instrument Corp.) was used for planar bilayer experiments. The analogue output was filtered with an 8-pole

Bessel filter (Frequency Devices, model 902) and digitized with a 333 kHz digitizer (Axon Instruments, Digidata 1200A). Data acquisition was controlled by the pClamp8 software package (Axon Instruments). Data were collected at 10 kHz, analogue filtered at 1 kHz, and digitally filtered at 100 Hz (**2**, **4**) or 50 Hz (**3**). The headstage and the bilayer chamber (3 mL polystyrene cuvette with 250 μm diameter aperture held in a 5 mL PVC holder) were placed on a floating table and electrically shielded by a grounded aluminum Faraday cage. Agar salt bridges (2 M KNO<sub>3</sub> in 1% Agar) were used to stabilize junction potentials and were employed between the electrolyte in each well of the cell and Ag/AgCl electrodes. Electrolyte solutions were prepared from high purity salts and Nano-pure water (resistivity greater than 17.9 Ω cm). A stock solution of diphtanoyl phosphatidylcholine (diPhyPC) in chloroform (Avanti Polar Lipids; shipped on dry ice) was divided into sealed glass vials under an argon atmosphere and stored at –12 °C. For use in an experiment, the vial was held at vacuum for 2 h before being diluted with decane to give a solution concentration of 25 mg/mL lipid. Bilayers were formed by either brushing or dipping as described previously.<sup>24</sup> Briefly, after lipid in decane had been introduced by brushing, a lipid/decane film formed on the surface of the electrolyte, and bilayers could then be formed by withdrawal of 2–3 mL of electrolyte from the cell holder by syringe to expose one face of the aperture to the air–water interface held in the cell holder, followed by reintroduction of the electrolyte to oppose monolayers across the aperture in the cuvette. Bilayer quality was monitored via the capacitance and stability under applied potential, using the criteria previously described.<sup>24</sup> All experiments utilized bilayers that were apparently stable at ±100 mV for periods of 20 min or more. Aliquots (1–5 μL) of transporter solutions (**2**, 7.2 mM in DMSO; **3**, 6.6 mM in DMSO; **4**, 6.4 mM in methanol) were injected with a microliter syringe as closely as possible to the bilayer in the free well of the cuvette holder (cis side). The measured voltage was applied with respect to the trans (cuvette) side of the bilayer, making the trans side the relative ground. Digitized data files were analyzed using the pClamp8 suite of programs and imported to Origin 6.1 for additional analysis and plotting. Single-ion activity coefficients were calculated by an extended Debye–Huckel method.<sup>35</sup>

**Acknowledgment.** The ongoing support of the Natural Science and Engineering Research Council of Canada and of the University of Victoria is gratefully acknowledged.

**Supporting Information Available:** Copies of <sup>1</sup>H and <sup>13</sup>C NMR spectra of the new compounds prepared. This material is available free of charge via the Internet at <http://pubs.acs.org>.

JO026415F

(35) Meier, P. C. *Anal. Chim. Acta* **1982**, *136*, 363–368.